arXiv:1401.0723v1 [cond-mat.mes-hall] 3 Jan 2014

Spin-Transfer-Torque Driven Magneto-Logic Gates Using Nano Spin-Valve Pillars

C. Sanid and S. Murugesh*
Department of Physics, Indian Institute of Space Science and Technology, Trivandrum - 695 547, India.

We propose model magneto-logic NOR and NAND gates using a spin valve pillar, wherein the logical operation is induced by spin-polarized currents which also form the logical inputs. The operation is facilitated by the simultaneous presence of a constant *controlling* magnetic field. The same spin-valve assembly can also be used as a magnetic memory unit. We identify regions in the parameter space of the system where the logical operations can be effectively performed. The proposed gates retain the non-volatility of a magnetic random access memory (MRAM). We verify the functioning of the gate by numerically simulating its dynamics, governed by the appropriate Landau-Lifshitz-Gilbert equation with the spin-transfer torque term. The flipping time for the logical states is estimated to be within nano seconds.

* murugesh@iist.ac.in

I. INTRODUCTION

Following the discovery of the celebrated giant magneto-resistance (GMR) effect and the development of spin-valve structures, a reciprocal phenomenon of GMR, a torque on the spin magnetization induced by spin polarized currents, was independently predicted by Slonczewski and Berger[1, 2]. In this spin-transfer torque (STT) effect a spin polarized current flowing perpendicular to a thin ferromagnet generates a torque strong enough to reorient its magnetization. Information coded in the form of macrospin of the magnetic layer, considered as a monodomain, is thus amenable to manipulation using spin-polarized currents [3, 4]. The extensive theoretical and experimental studies on spin valve geometries that followed brought into light two especially important phenomena relevant to magnetic storage technology and spintronics - current induced magnetization switching and self-sustained microwave oscillations in the nanopillar devices[5–9].

The aspect of *non-volatility*, fundamentally inherent in the system, and the significant reduction in power consumption have prompted the development of spin-valves as memory devices. The earlier proposals, however, were based on a field induced magnetic switching(FIMS) approach for writing data, which uses two orthogonal pulses of magnetic filed to achieve writing. Magnetic random access memory (MRAM) models based on current induced magnetic switching (CIMS), wherein STT phenomenon forms the core, have since been proposed. Apart from the more obvious application as plain memory storage devices, spin valve based magneto-logic devices have also been attempted in the recent past. FIMS based field programmable logic gates using GMR elements were proposed by Hassoun *et al.*[10], wherein the type of the logical operation to be performed can be altered by additional fields. Further models have also been suggested where the logical state of the GMR unit is manipulated using FIMS [11–15]. Similar programmable models based on spin valve magneto-logic devices are also known in literature[16–18]. These later models, based on CIMS, involve additional spin-valve elements that together form a single logical unit, or more than one current carrying plate capable of generating fields in orthogonal directions. Besides, in these models, bi-polar currents were crucial in writing or manipulating data. Invariably, this requires a more complex architecture than is required for a simple magnetic memory unit.

In this paper we propose alternative magneto-logic NAND and NOR gate models, wherein the logical operation is performed through CIMS in the presence of a controlling field. Apart from the simplicity in the architecture, the models also carry the advantage that they can be used as plain memory elements in a MRAM. They consist of a single spin-valve pillar and no additional elements, than those required for its functioning as a memory unit, are required to enhance its role as a logical gate. In the proposed models we use STT for writing, while the magnetic field is held constant in magnitude (positive for NOR and negative for NAND gate) and required only during the logical operation. Thus the applied field acts as a control switch for the gates. The gates are also non-volatile, as naturally expected in a magneto-logic device.

II. SPIN-VALVE PILLAR GEOMETRY AND THE GOVERNING LANDAU-LIFSHITZ-GILBERT EQUATION

The system under consideration is a regular spin valve primarily consisting of a conducting layer sandwiched between two ferromagnetic layers, one pinned and the other free, with the magnetization in the pinned layer parallel to the plane of the free layer - a geometry that is well studied[7, 19, 20]. Further, the free layer is also subject to a constant Oersted field, by a conducting plate carrying current. The dynamics of the macrospin magnetization of the free layer is governed by the Landau-Lifshitz-Gilbert (LLG) equation with the STT term, whose dimensionless form is given by[9, 21]

$$\frac{\partial \mathbf{m}}{\partial t} - \alpha \mathbf{m} \times \frac{\partial \mathbf{m}}{\partial t} = -\mathbf{m} \times \mathbf{H}_{eff}, \tag{1}$$

where

$$\mathbf{H}_{eff} = \left(\mathbf{h}_{eff} - \beta \frac{\mathbf{m} \times \mathbf{e}_p}{1 + c_p \mathbf{m} \cdot \mathbf{e}_p} \right).$$

The free-layer magnetization $\mathbf{m}$ and the effective field $\mathbf{h}_{eff}$ are normalized by the saturation magnetization M_s. Time is measured in units of $(\gamma M_s)^{-1}$, where γ is the gyromagnetic ratio (for Co layers, this implies time scales in the order of picoseconds). The constant α is the damping factor and unit vector $\mathbf{e}_p$ is the direction of pinning ($\hat{\mathbf{x}}$ in our case, and in plane). The other constant c_p $(1/3 \leq c_p \leq 1)$ is a function of degree of spin polarization P $(0 \leq P \leq 1)$:

$$c_p = \frac{(1+P)^3}{3(1+P)^3 - 16P^{3/2}} \tag{2}$$

In the numerical calculations that follow we have used the typical value of $P = 0.3$. The phase diagrams, to be discussed in the next section, do exhibit minor variations with change in the value of P, but do not alter our results much. For, as can be seen from eq. (2), c_p is a small number compared to 1 for all realistic values of P. The parameter β is proportional to the spin current density (typically of the order of 10^{-2} for Co layers, with current densities $\sim 10^8$ A/cm^2). The effective field is given by

$$\mathbf{h}_{eff} = h_{ax}\hat{\mathbf{x}} - (D_x m_x \hat{\mathbf{x}} + D_y m_y \hat{\mathbf{y}} + D_z m_z \hat{\mathbf{z}}),$$

where $h_{ax}\hat{\mathbf{x}}$ is the external field and D_is$(i = x, y, z)$ are constants that reflect the crystal shape and anisotropy effects. Particularly, we chose our film such that the anisotropy is in-plane, and also lies along the x-axis. The plane of the free layer is chosen to be the $x - y$ plane. With this choice $D_i s$ are such that $D_x < D_y < D_z$, making $\hat{\mathbf{x}}$ the free-layer easy axis.

III. GEOMETRY OF FIXED POINTS AND MAGNETO-LOGIC GATES

For our choice of geometry, described in the previous section, the magnetization in the free layer exhibits a variety of dynamics in different regions of the $h_{ax} - j\,(\equiv \beta/\alpha)$ parameter space - such as in-plane limit cycles (O) and symmetric out-of-plane limit cycles (O^2), and stable fixed points parallel to $\hat{\mathbf{x}}$(P), parallel to $-\hat{\mathbf{x}}$(A) and symmetric out-of-plane stable fixed points (S^2)[21, 22]. In Fig. 1 we show two specific ranges where the models we propose can perform the desired logical operations. The type of dynamics in the different regions of the parameter space is identified here by numerically simulating the LLG equation eq. (1). These results clearly agree with those obtained analytically in [21, 22].

A. Logic NOR gate

For the logical NOR gate, we shall choose the applied field (whenever non-zero) to be positive and $|h_{ax}| > D_z - D_x$. For this choice, there can at best be only one stable fixed point, lying along either $\pm\hat{\mathbf{x}}$ directions depending on the values of h_{ax} and j. For a given set of values of the system parameters, D_is and α, fixed points corresponding to four scenarios of special interest to us in designing our NOR gate are shown in Fig. 2. When j is held below a certain threshold value, and $|h_{ax}| > D_z - D_x$, $\mathbf{m} = \hat{\mathbf{x}}$ is the only stable fixed point, while $-\hat{\mathbf{x}}$ is unstable. For j beyond a certain upper threshold value j_{c1}, with h_{ax} held at the same value, the situation reverses, with $\hat{\mathbf{x}}$ becoming unstable and $-\hat{\mathbf{x}}$ becoming the stable point. When $h_{ax} = 0 = j$, both $\pm\hat{\mathbf{x}}$ become stable on account of the anisotropy field along the $\mathbf{x}$ axis. Finally, when h_{ax} is held at zero, but $j > j_{c1}$, the scenario in Fig. 2(b) repeats, with $-\hat{\mathbf{x}}$ stable and $\hat{\mathbf{x}}$ unstable.

A numerical simulation of the governing LLG equation with the STT term, eq. (1), shows the expected magnetization switching in conformity with Fig. 2. We choose the system parameters $\alpha = 0.01$, $D_x = -0.034$, $D_y = 0$, and $D_z = 0.68$ (as in ref. [7]). Taking the value of saturation magnetization, M_s, to be that of Co (1.4×10^6 A/m), it effectively implies a time scale of 3.2 ps. The switching time due to the spin-current is roughly 0.2 ns, while that due to the magnetic field is slower, at nearly 0.7 ns, accompanied by a ringing effect. This delay and ringing effect are well understood to be due to the fact that, even with $\alpha = 0$, a spin-transfer-torque leads to both precession and dissipation whereas a magnetic field alone can only cause a precession of magnetization vector about the applied field[23]. Field induced switching is thus exclusively due to the damping factor, leading to a longer switching time, consequently. A longer switching time invariably implies more precession meanwhile, causing the ringing effect. In Figure 3, we show the dynamics of the x component of the normalized magnetization vector $\mathbf{m}$ as the field and current are switched through various possible combinations. The current density used is of the order of 10^8 A/cm^2, and the field h_{ax} is of the order of 10^6 A/m. Such a magnitude for the applied field, although frequently used (see, for instance ref. [7]), is substantially high for real world applications. Magnetic tunnel junctions (MTJs) have proved themselves to be more worthwhile candidates as MRAMs, with their operability at much lower spin-current and field amplitudes, and higher ferromagnetic to anti-ferromagnetic current ratios[24–26]. Although the STT phenomenon in MTJs and that in spin-valve pillars display several qualitative similarities, MTJs are hampered by the lack of an appropriate mathematical model to describe their dynamics. We believe results presented in this paper will be of relevance in MTJs too and may possibly be reproduced. Our numerical simulations show that the model presented is robust with respect to errors that may creep in through two of the system parameters - variations in the degree of polarization, and in plane anisotropy fields in the form of D_x. We have varied these values upto 10% and yet noticed no percievable difference in the phase diagram. The chosen values of $j_i' s$ $(0.6 j_{c1})$ provides enough room for errors arising out of fluctuations. Further, we recall that as long as the condition $|h_{ax}| > D_z - D_x$ is satisfied we have the two desired fixed points, enabling the required logical operation.

We make use of the first three scenarios (Figs. 2(a)-2(c)) to construct the universal NOR gate, which retains the non-volatility of spin based memory devices. Let j_1 and j_2 be currents that form inputs to the logic gate, and each take either of the two values - *zero*, or some value j little over j_{c1}. We shall identify these values of the current with the logical input states 0 and 1, respectively. Both currents j_1 and j_2 are fed together into the spin-valve from the pinned layer end. The field h_{ax} is held fixed throughout the logical operation (represented henceforth simply as h_{ax} =1), and acting as a controlling field. When the currents $j_{1,2}$ are both zero, the magnetization $\mathbf{m}$ orients itself along $\hat{\mathbf{x}}$, the only stable fixed point. This corresponds to the low resistance state, being *parallel* to the pinned layer magnetization, which we read as the logical state 1. When either, or both, of the currents $j_{1,2}$ is greater than j_{c1}, the torque is sufficient enough to flip the spin $\mathbf{m}$ from any direction to the new stable fixed point $-\hat{\mathbf{x}}$ (the high resistance *anti-parallel* state 0). The following truth table of the NOR gate is thus obtained (see Table 1). When the field h_{ax} and the currents $j_{1,2}$ are all switched off, both $\pm\hat{\mathbf{x}}$ are equally good stable fixed points due to the anisotropy field along the $\mathbf{x}$ axis. Prior value of magnetization is therefore retained, and the gate carries the non-volatility of the MRAM.

h_{ax}	j_1	j_2	$\mathbf{m}$ (logical state)
1	0	0	$\hat{\mathbf{x}}$ (1)
1	1	0	$-\hat{\mathbf{x}}$ (0)
1	0	1	$-\hat{\mathbf{x}}$ (0)
1	1	1	$-\hat{\mathbf{x}}$ (0)

TABLE I. The truth table for NOR gate. The applied field is always held constant through out the operation ($|h_{ax}| > D_z - D_x$) indicated by $h_{ax} = 1$. The currents $j_{1,2}$ take either a value greater than j_{c1}, indicated as the logical input 1, or zero taken as input 0.

The nature of fixed points depicted in Figs. 2(a), 2(c), and 2(d), show that the same valve assembly can also be used as a plain memory device. To this end we shall use a single current input, j, to the spin-valve as opposed to the two inputs for the gate assembly. *Writing* the data bit 1 is then enabled with a applied field $h_{ax} = 1$ and current $j = 0$. Similarly the bit 0 is written when $h_{ax} = 0$ and $j = 1$. The two stable fixed points, as shown in Fig. 2(c), then ensure that the magnetization, or *data*, is retained in the absence of both the current and field, preserving non-volatility. A schematic representation of the logical NOR gate for a choice of input currents, and with control field $h_{ax} = 1$, is shown in Fig. 4.

B. Logic NAND gate

We now look at the fixed points corresponding to another region of the $h_{ax} - j$ parameter space [Fig. 1(b)]. The applied field h_{ax} is chosen to be *negative* (again, whenever non-zero), while still satisfying the earlier condition that $|h_{ax}| > D_z - D_x$, and the current j assumes either of the three values, *zero*, $0.6j_{c2}$ or $1.2j_{c2}$ [where j_{c2} is indicated in Fig. 1(b)]. Notice that j_{c2} is *negative*, implying a current sent in the opposite direction along the pillar. The fixed points corresponding to different combinations of h_{ax} and j are shown in Fig. 5. We shall denote the above mentioned negative value of the magnetic field as $h_{ax} = -1$. For the NAND gate we shall take the current value $j = 0$, and $j = 0.6j_{c2}$ as the logical inputs 0 and 1, respectively. In the absence of both current and field, the stable fixed points are $\pm\hat{\mathbf{x}}$, as in Fig. 2(c). When the field $h_{ax} = -1$ and the current is either 0 or 1, $\hat{\mathbf{m}} = -\hat{\mathbf{x}}$ is the only stable fixed point while $\hat{\mathbf{m}} = \hat{\mathbf{x}}$ becomes unstable. When the current value $j = 1.2j_{c2}$, however, the situation reverses, with $\hat{\mathbf{x}}$ becoming stable, and $-\hat{\mathbf{x}}$ unstable. A numerical simulation, analogous to Figure 3, for these new values of h_{ax} and j is shown in Figure 5, with results as expected.

As in the case of the NOR gate, let j_1 and j_2 be the currents fed together, and each take values 0 or 1 (now corresponding to negative currents). The magnetic field is held constant at $h_{ax} = -1$ all along the logical operation. For the logical NAND gate we adopt the opposite convention, interpreting the high-resistance state ($\hat{\mathbf{m}} = -\hat{\mathbf{x}}$) as the logical state 1, and the low-resistance state as 0. The following truth table of the NAND operation is thus realized (Table 2). As both $\pm\hat{\mathbf{x}}$ are stable fixed points in the absence of current and magnetic field [Fig. 2(c)], non-volatility is ensured.

h_{ax}	j_1	j_2	**m** (logical state)
-1	0	0	$-\hat{\mathbf{x}}$ (1)
-1	1	0	$-\hat{\mathbf{x}}$ (1)
-1	0	1	$-\hat{\mathbf{x}}$ (1)
-1	1	1	$\hat{\mathbf{x}}$ (0)

TABLE II. The truth table for NAND gate. As earlier, the applied field is always held constant through out the operation, though negative. The currents $j_{1,2}$ take either of the two values $0.6j_{c2}$ - the logical input 1, or zero taken as input 0.

IV. SUMMARY

In summary, we have proposed spin-valve based magneto-logic NOR and NAND gate assemblies, which render themselves to the dual role of universal gate and a magnetic memory. A constant applied magnetic field parallel to the pinned layer magnetization acts as a control for the logic gate operation, while spin-currents are fed in as the logical inputs. The same pillar geometry is used for both the NOR and NAND gates, and also doubles as a magnetic memory device.

[1] J. C. Slonczewski: J. Magn. Magn. Mater. **159** (1996) L1.
[2] L. Berger: Phys. Rev. B **54** (1996) 9353.
[3] M. D. Stiles and J. Miltat: T. Appl. Phys. **101** (2006) 225.
[4] S. A. Wolf, A. Y. Chtchelkanova, and D. M. Treger: IBM J. Res. & Dev. **50** (2006) 101.
[5] E. B. Myers, D. C. Ralph, J. A. Katine, R. N. Louie, and R. A. Buhrman: Science **285** (1999) 867.
[6] J. Grollier, V. Cros, A. Hamzic, J. M. George, H. Jarrfés, A. Fert, G. Faini, J. B. Youssef, and H. Legall: Appl. Phys. Lett. **78** (2001) 3663.
[7] S. I. Kiselev, J. C. Sankey, I. N. Krivorotov, N. C. Emley, R. J. Schoelkopf, R. A. Buhrman, and D. C. Ralph: Nature **425** (2003) 380.
[8] W. H. Rippard, M. R. Pufall, S. Kaka, S. E. Russek and T. J. Silva: Phys. Rev. Lett. **92** (2004) 027201.
[9] D. V. Berkov and J. Miltat: J. Magn. Magn. Mater. **320** (2008) 1238.
[10] M. W. Hassoun, W. C. Black Jr., E. K. F. Lee, and R. L. Geiger: IEEE Trans. Magn. **33** (1997) 3307.
[11] R. Richter, H. Boeve, L. Bär, J. Bangert, U. Klostermann, J. Wecker, and G. Reiss: J. Magn. Magn. Mater. **240** (2002) 127.
[12] A. Ney, C. Pampuch, R. Koch, and K. H. Ploog: Nature **425** (2003) 485.
[13] A. Ney and J. S. Harris, Jr.: Appl. Phys. Lett. **86** (2005) 013502.
[14] J. Wang, H. Meng, and J.-P. Wang: J. Appl. Phys. **97** (2005) 10D509.
[15] S. Lee, S. Chao, S. Lee, and H. Shin: IEEE Trans. Electron Devices **54** (2007) 2040.
[16] W. Zhao, E. Belhaire, and C. Chappert: Proc. 7th IEEE Int. Conf. Design and Test of Integrated Systems in Nanoscale Technology, 2007, p. 399.
[17] H. Dery, P. Dalal, L. Cywinski, and L. J. Sham: Nature **447** (2007) 573.
[18] B. Buford, A. Jander, and P. Dhagat: arXiv:1101.3222v1.
[19] F. J. Albert, J. A. Katine, and R. A. Buhrman: Appl. Phys. Lett. **77** (2000) 3809.
[20] S. Mangin, D. Ravelosona, J. A. Katine, M. J. Carey, B. D. Terris and E. E. Fullerton: Nat. Mater. **5** (2006) 211.
[21] G. Bertotti, C. Serpico, I. D. Mayergoyz, A. Magni, M. d'Aquino, and R. Bonin: Phys. Rev. Lett. **94** (2005) 127206.
[22] G. Bertotti, I. Mayergoyz and C. Serpico: *Nonlinear Magnetization Dynamics in Nanosystems* (Elsevier, Amsterdam, 2008).
[23] S. Murugesh and M. Lakshmanan: Chaos, Solitons Fractals **41** (2009) 2773.
[24] A. Kalistov, M. Chshiev, I. Theodonis, N. Kioussis, and W. H. Butler: Phys. Rev. B. **79** (2009) 174416.
[25] S. Parkin, J. Xin, C. Kaiser, A. Panchula, K. Roche, and M. Samant: Prof. IEEE **91** (2003) 661.
[26] J. Daughton: J. Appl. Phys. **81** (1997) 3758.

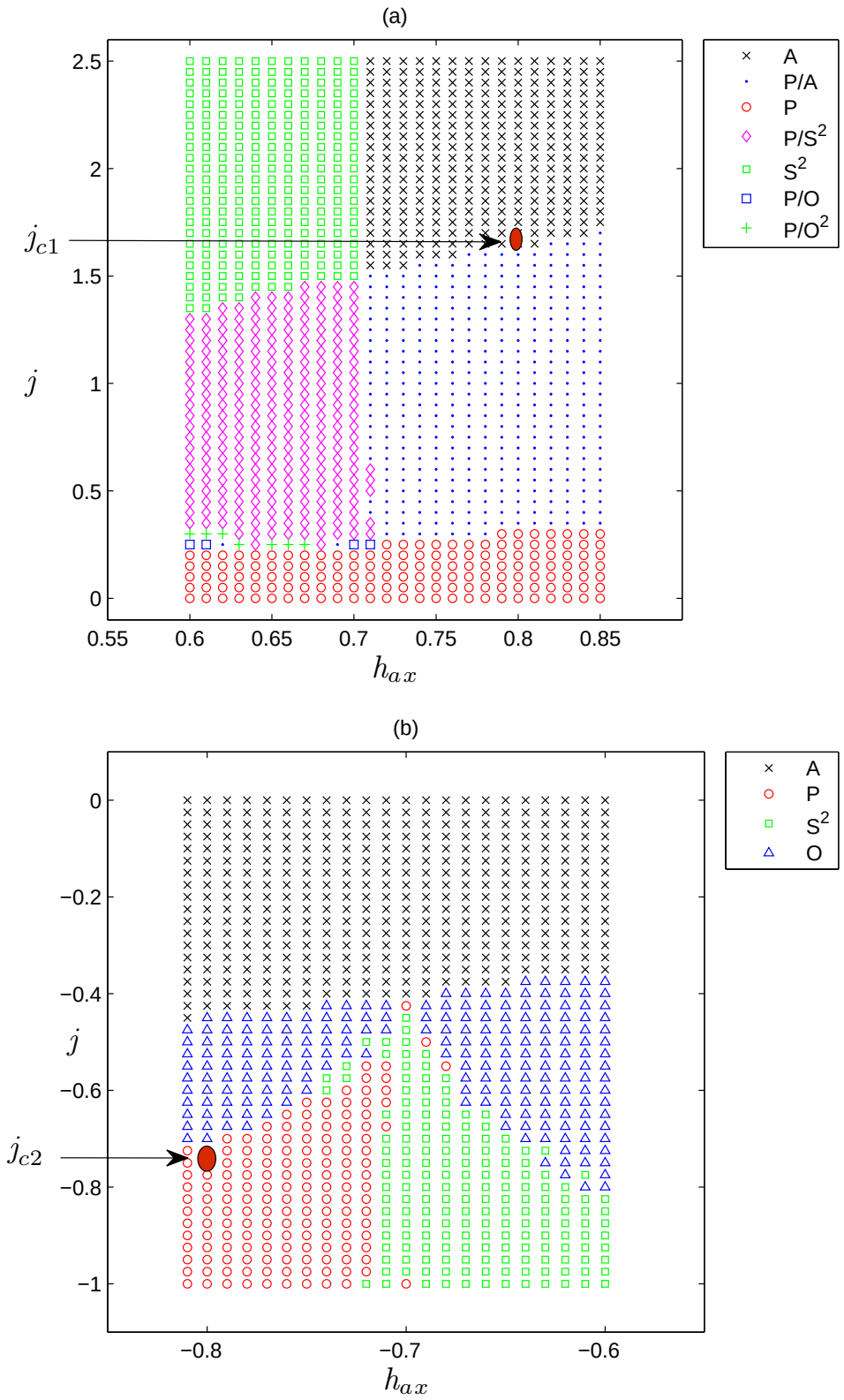

FIG. 1. Phase diagram in the $h_{ax} - j$ space, in regions relevant for the (a) NOR and (b) NAND gates. The system displays limit cycles(O), symmetric out-of-plane limit cycles (O^2), stable fixed points parallel to $\hat{\mathbf{x}}$(P) or $-\hat{\mathbf{x}}$(A), and symmetric out-of-plane stable fixed points (S^2). The critical value of the current and the field used for our models (j_{c1} and j_{c2}) are circled in the two figures.

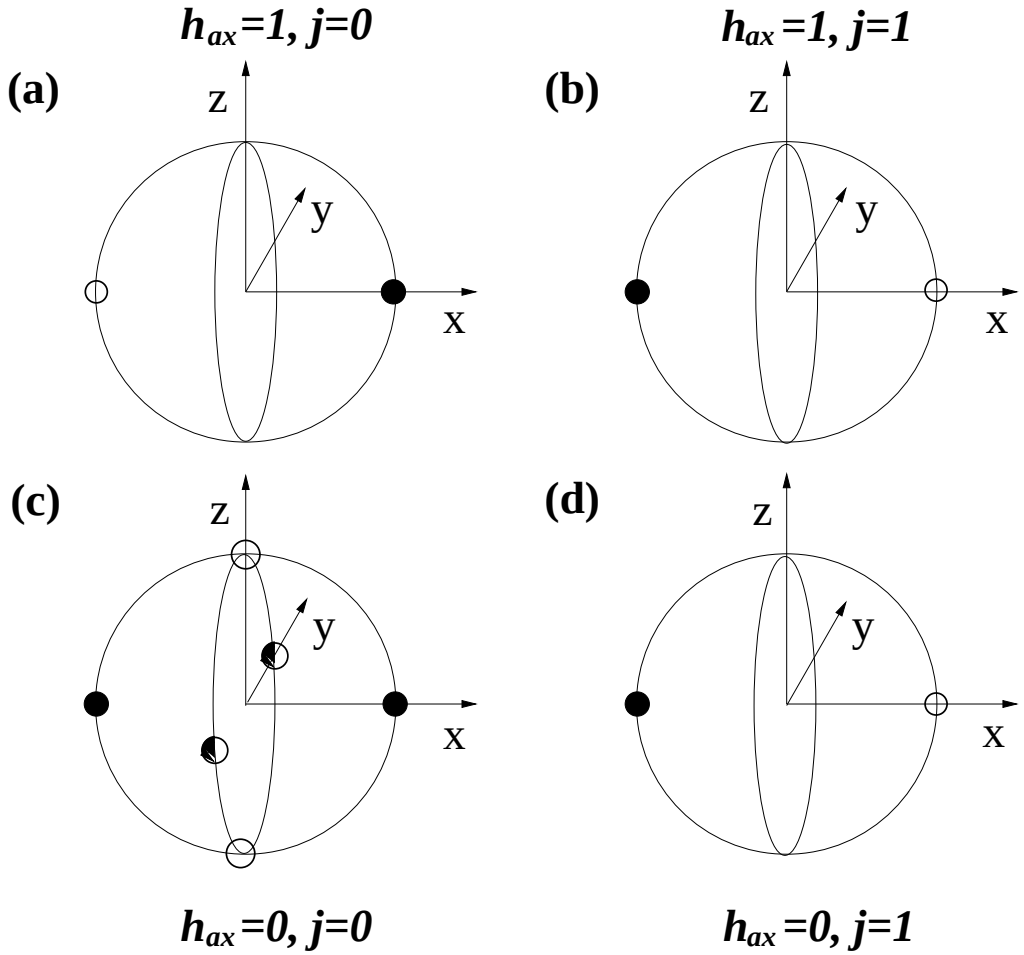

FIG. 2. Fixed points for four different cases. For convenience, we have indicated the fixed value of the applied field we have used through out, satisfying the condition $|h_{ax}| > D_z - D_x$, as h_{ax} =1. Similarly the value for $j\,(> j_{c1})$, is indicated by $j = 1$. (a) $h_{ax} = 1,\ j = 0$, (b) $h_{ax} = 1,\ j = 1$, (c) $h_{ax} = 0,\ j = 0$, and (d) $h_{ax} = 0,\ j = 1$. Stable fixed points are indicated by filled dots, and unstable fixed points by unfilled dots. For $h_{ax} = 0 = j$, there arise six fixed points, two of which are saddles indicated by half filled dots, and both $\pm\hat{\mathbf{x}}$ are stable fixed points.

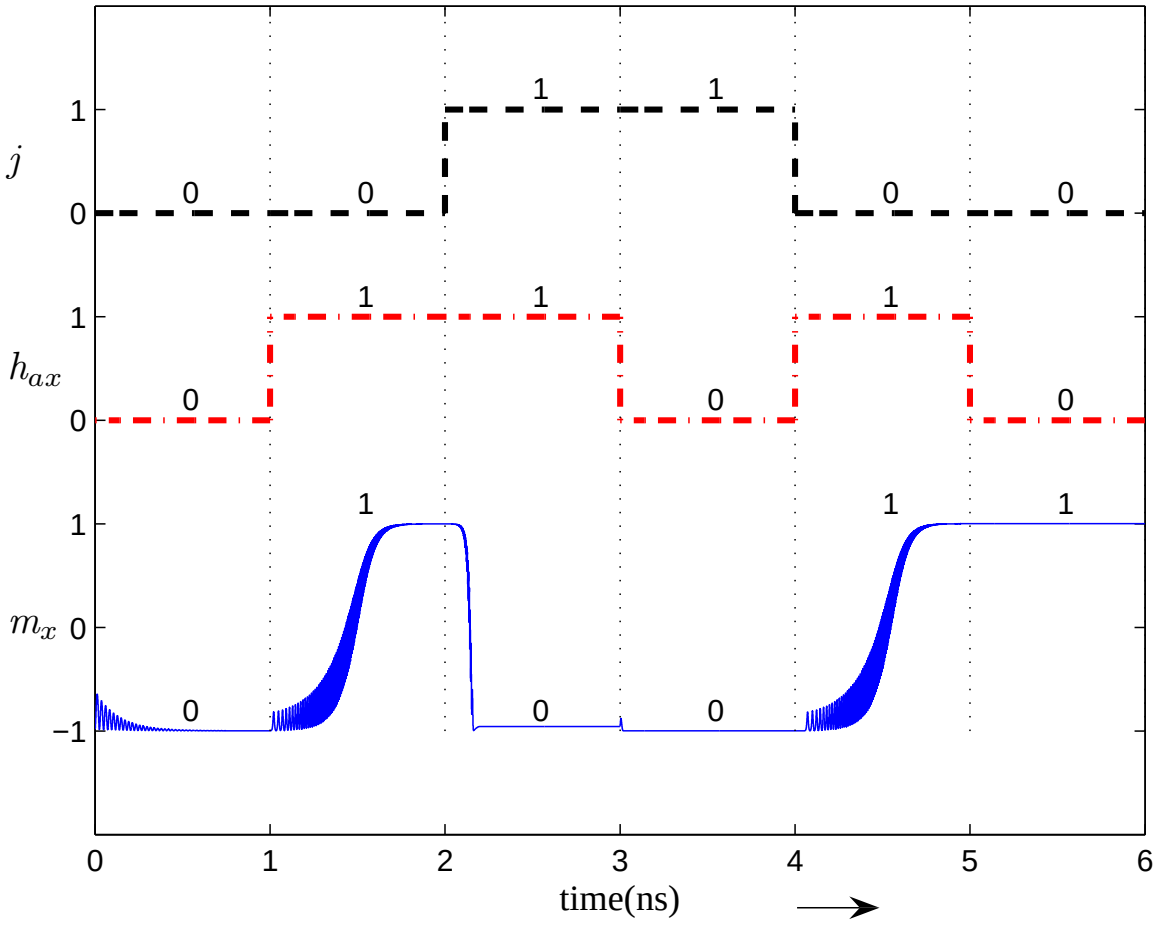

FIG. 3. Time evolution of m_x (bottom) as the applied field h_{ax} (middle) and j (top) are flipped through various combinations, with the interpreted logical state. The initial orientation of $\mathbf{m}$ is chosen arbitrarily. For the case $h_{ax} = 0 = j$, both $\pm\hat{\mathbf{x}}$ are stable fixed points, and the magnetization relaxes to the nearest of the two directions-$m_x = -1$ initially, and $m_x = +1$ finally.

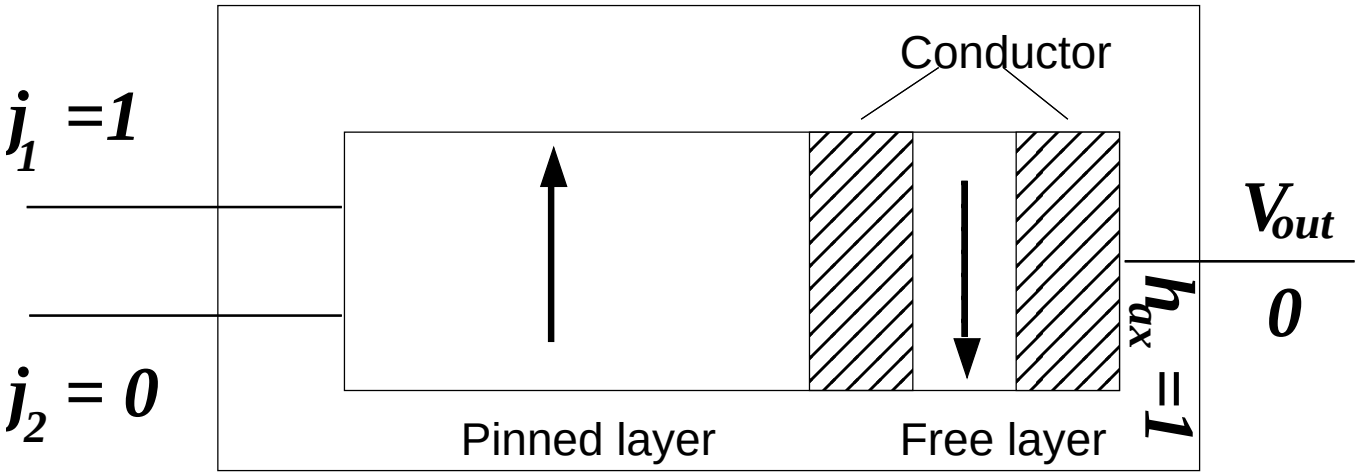

FIG. 4. A schematic diagram of the NOR gate, with the relevant portion of the spin-valve pillar, and a specific set of values for the input currents $j_i's$ and the control field h_{ax}. The logical output is interpreted from the value of the potential V_{out}, either high (state 1) or low (state 0).

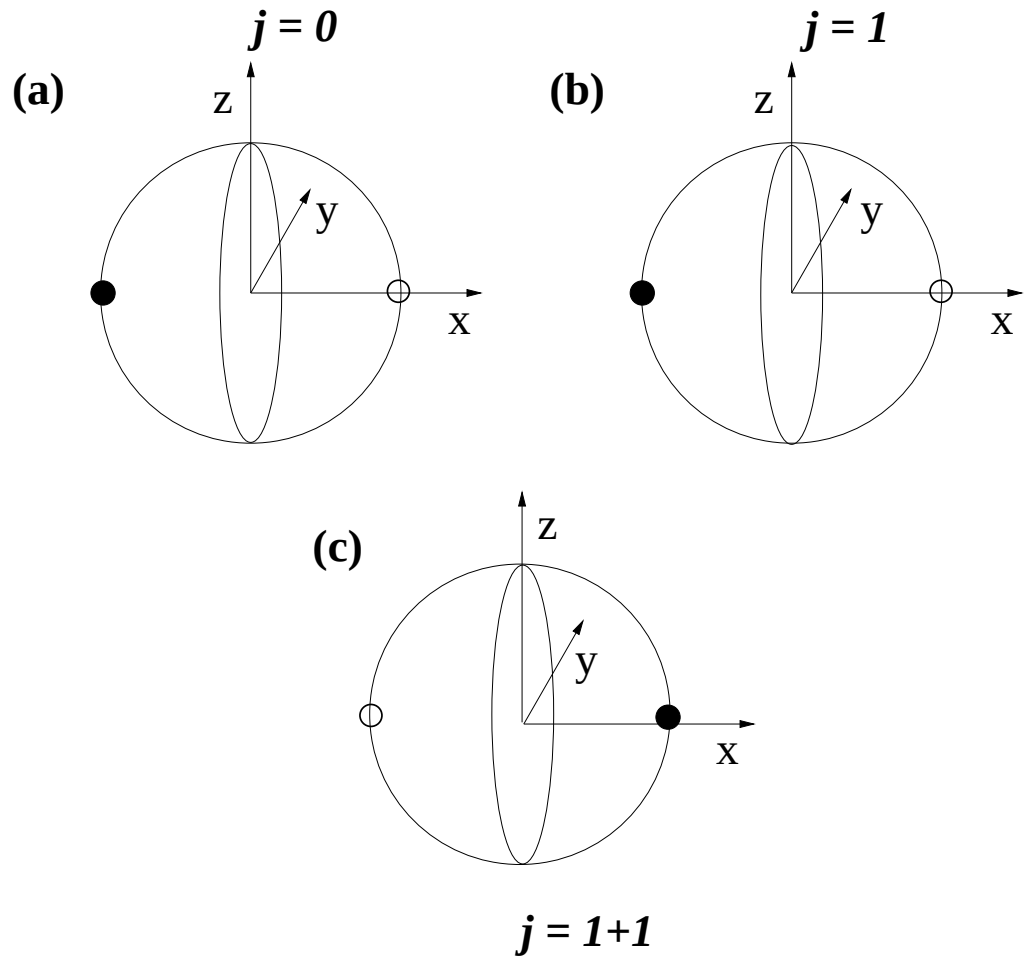

FIG. 5. Fixed points for three different values of the current j, (a) $j = 0$, (b) $j = 1\,(0.6j_{c2})$ and (c) $j = 1 + 1\,(1.2j_{c2})$. The applied field h_{ax} is the same, and is negative with $|h_{ax}| > D_z - D_x$. When both field and current are zero, the fixed points are the same as in Fig. 1(c).

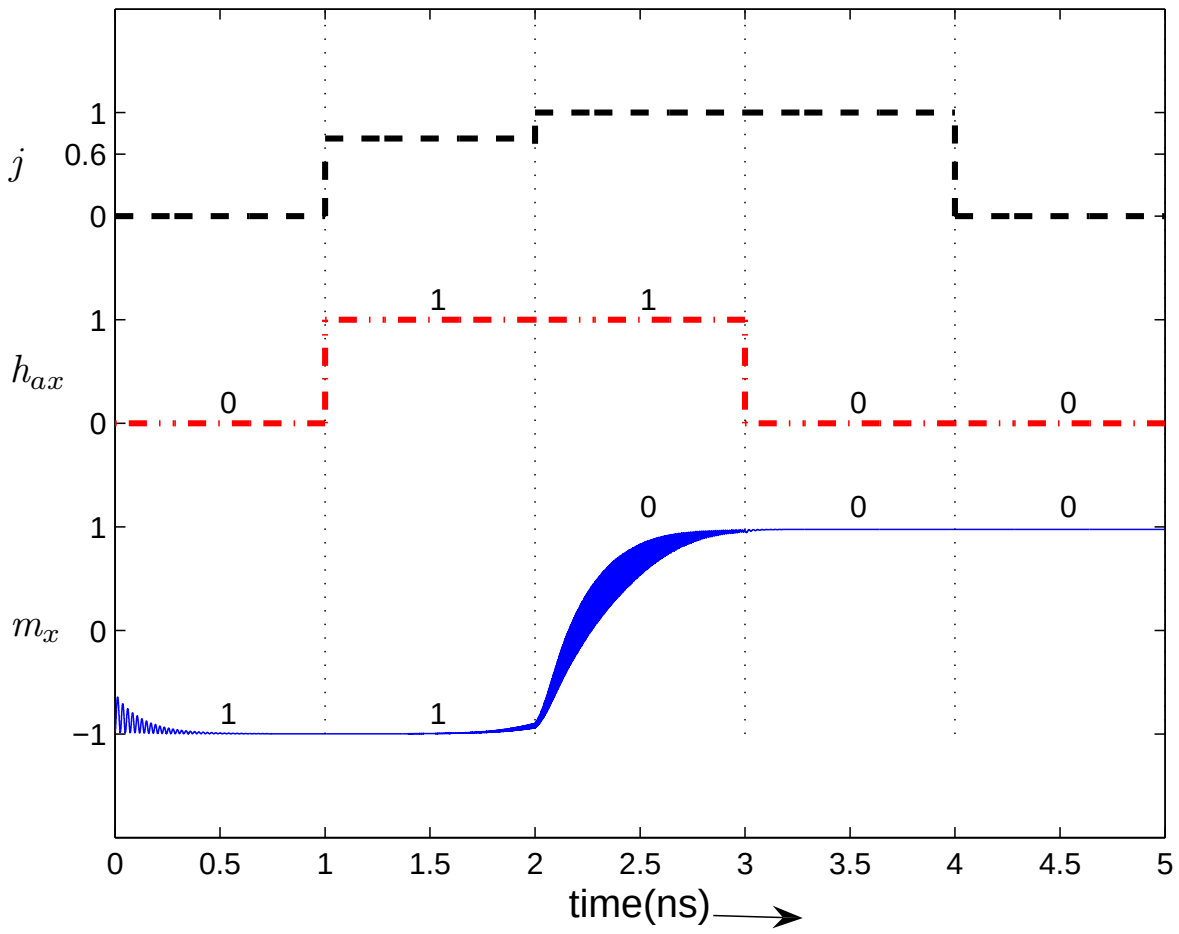

FIG. 6. Time evolution of m_x (bottom) as the applied field h_{ax} (middle) and j (top) are flipped through various combinations, relevant to the NAND gate. The interpreted logical state is indicated over the respective m_x values. For the parameter values chosen, the switching time is within 1 ns.